Femtosecond correlated optical reactivity and scanning tunneling microscopy studies of metal surfaces

Mark J. Feldstein[a] and Norbert F. Scherer[b]

[a]Center for Biomolecular Science and Engineering,
Naval Research Laboratory, Washington, DC 20375
[b]Department of Chemistry and the James Franck Institute, The University of Chicago,
Chicago, IL 60637

ABSTRACT

A new experimental technique, correlated optical reactivity and scanning tunneling microscopy (CORSTM), is shown to be a uniquely powerful tool for the study of spatially localized reactivity of surfaces. In particular, CORSTM measurements directly correlate electromagnetic field enhancements that affect chemical dynamics and reactivity with surface topography on the length scale of a few nanometers. These measurements are based on the detection of surface plasmon polariton mediated multi-photon ionization (SPP-MPI) from metal surfaces using ultrafast optical excitation and scanning probe microscopy photoelectron detection. The CORSTM approach is extended to a pump-probe scheme facilitating spatially localized measurement of hot electron dynamics. The experimental results provide direct confirmation of the optimal structural topographies for surface enhanced spectroscopy predicted by electromagnetic theories. CORSTM will provide a better understanding of phenomena that involve plasmons through the direct measurement of structure-function correlations.

1. INTRODUCTION

The relationship between structure and functionality (or reactivity) is an underlying principle for the molecular biological and chemical sciences. This concept is equally relevant for phenomena occurring on length scales exceeding the molecular. The detection of quantized conduction in nanometer to micron-size structures is an example from the area of mesoscopic physics.[1] The structure-function paradigm also applies to observables related to excitation of collective modes of materials as exemplified in the sensitivity of surface plasmon polaritons (SPP) to the structural and chemical nature of the interface.[2] Because of their inherent surface sensitivity, the properties of SPP's in thin metal films have been exploited in a number of fields of chemistry and biology. These include surface enhanced Raman scattering (SERS),[3] plasmon resonance spectroscopy (PRS; chemical and biological),[4] plasmon imaging by Photon STM and plasmon resonance microscopy,[5] and the plasmon response of colloidal metal particles and films.[6]

The coupling of photons into the SPP mode of a material and the resultant large local electromagnetic fields are central to realizing surface enhanced spectroscopy (SES). Roughened metal surfaces have been of particular scientific interest since their discovery as good substrates for SES.[7,8] Subsequent experimental emphasis has been on preparing and characterizing ideal SES substrates for investigation of sub-monolayer adsorbate coverages with enhanced sensitivity.[3] Experimental support for the types of surface topographies that give rise to the largest predicted field enhancements came through measurements of SERS signals from structured surface sites.[3,8,9] Rough surfaces result in greater signal enhancement over smooth ones,[9] metal islands resulting from the formation of regular features (*i.e.,* hemisphereoids or spheroids) in quasi-periodic patterns yield greater enhancements still.[3] Colloidal Au particles tethered to substrates also cause large SERS enhancements.[6] These studies have only been able to correlate an average or representative surface structure with measured enhancements. However, two very recent studies have reported the detection of Raman scattering from single metal particles.[10]

By contrast, theoretical studies of SES have established the local field enhancements for particular geometries on model surfaces;[8,11] the field enhancements are, in general, a direct consequence of SPP excitation. These high local electromagnetic fields affect the local propensity for photochemical reactivity, especially for higher order processes like

multi-photon ionization (MPI). MPI from metal films is, therefore, a representative measure of the electromagnetic contribution to SES processes since, under appropriate conditions, it is a direct result of SPP excitation.[9,12,13] Thus, the spatially-localized measurement of SPP-mediated MPI (SPP-MPI) might be used to test and examine electromagnetic field enhancements.

This paper is the first report of measurements that directly correlate metal structural features with plasmon-induced reactivity and the near-field local plasmon dynamics on femtosecond time scales and nanometer length scales. Correlated optical reactivity and scanning tunneling microscopy (CORSTM) measurements of rough metal surfaces are performed utilizing femtosecond pulse excitation of SPP's. A spatially localized probe (*i.e.*, STM) is used for simultaneous characterization of local surface topography and detection of the local electromagnetic field enhancement, the latter via SPP-MPI.

2. EXPERIMENTAL

Toward the goal of measuring the inherent geometric and topographic contributions in SES, that is, measuring the surface optical reactivity, it is necessary to rapidly couple energy into the surface and simultaneously characterize a direct product of the excitation. Based on the theory of electromagnetic enhancement at surfaces, SPP's are the most direct product of optical excitation. Using an STM, localized detection of SPP's has been reported by Möller *et al.*[14] using an ATR geometry and a low power, CW laser as the excitation source. SPP's were detected as additional, optically induced current through the STM. This signal was interpreted to be a result of optical rectification in the tunneling gap.[14,15]

The ATR geometry was also employed by Bozhevolnyi *et al.*[16] who used photon scanning tunneling microscopy (PSTM) and shear-force feedback microscopy to probe SPP and LSP fields. They report spatially localized enhancement ratios of 5:1 for island like structures on Au films at an air interface. They further report the measurement of signals related to SPP propagation along an internal interface. Several studies have shown,[14,16,17] that not only local detection of SPP's but the ATR geometry is ideal for investigating optical reactivity of a surface. This is the case since, among the benefits of direct, angularly tuned photon-SPP coupling, it allows for independent optical and scanning probe access to the surface thus eliminating shadowing and direct tip heating effects seen by others.[18] Similarly, results previously reported by this author,[12] as well as those reported herein, demonstrate the added advantages of time-resolved spectroscopy for imaging localized field enhancement and inherent surface optical reactivity.

The experimental schematic for CORSTM is shown in Figure 1. Experimental studies of the correlation of SPP-mediated reactivity and surface topography were conducted by optically exciting thin Ag films. The excitation geometry is based on the Kretschmann-Raether ATR configuration for photon-SPP momentum matching and coupling.[2] This geometry, with the pump and probe beams from the femtosecond pulse laser and STM interrogating the surface from opposite sides, facilitates excitation of a well defined SPP-mode without having to determine the waveguide behavior of the tip**.** The ~50 nm thick films were prepared by vacuum evaporation of Ag metal onto the hypotenuse of a right angle fused silica prism maintained at room temperature during deposition. The optical source is a home-built cavity-dumped Ti:Sapphire laser which produces pulses 30 fs in duration, centered at 780 nm, with energies of 20 nJ and a 50 KHz to 1 MHz repetition rate.[19] Focusing conditions yield peak intensities at the Ag film of nearly 1 GW/cm^2. The short duration pulses and high peak powers are critical for successful simultaneous measurement of the surface topography and reactivity.

The surface topography of the rough Ag films was determined by measuring the STM tunneling current,[20] recorded in "Current Imaging Mode",[21] using a home-built custom low pass (≤ 1 KHz) pre-amp with a gain of 10^9 V/A. Simultaneous determination of the photo-induced signal component is achieved by lockin amplifier demodulation of the output of a second pre-amp of custom design located in the STM head. Spatial resolution in these unique photo-induced surface reactivity measurements is achieved through the favorable interaction of several factors; the close proximity (~1 nm) of a sharp metallic tip to the surface, tip-surface field focusing,[22] and the highly nonlinear nature of the process being studied.[12] Finally, temporal resolution is achieved by an essentially standard 2-pulse pump-probe correlation technique.[12]

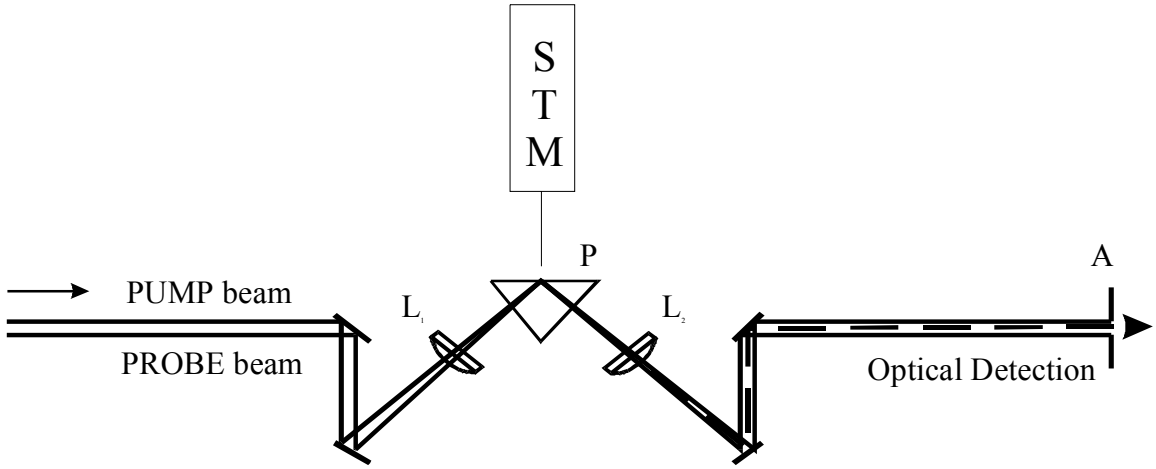

Figure 1. Experimental schematic showing the attenuated total internal reflection optical configuration and the juxtaposed STM. Pump and probe beams from the femtosecond pulse laser are focused and recollimated by lenses (L_1, L_2) onto the hypotenuse of a right angle prism (P) that has been coated with a thin metal film (Ag or Au). Detection of optical signals (fundamental, second harmonic, pump-probe; selected by aperture A) in the forward direction is also possible via detection synchronous with STM-induced perturbations of the SPP mode.[12] The STM tunneling current is separated into low and high frequency responses that are processed as the STM topography and the photo-induced signal, respectively. The STM tip is electrically insulated except at the apex.

3. RESULTS

Topography photo-reactivity correlations have been found for three qualitatively different surface structures. These experimental results are shown to be consistent with the predictions of SPP generation and electromagnetic field enhancement. Figure 2A shows the STM "topography" of a rough Ag film. The SPP-MPI photo-induced reactivity image shows structure different from that of the STM tunneling current image. The topography photo-reactivity correlation is evident in Fig. 2B. Here, the STM tunneling current image of Fig. 2A is shown with an overlay of the photo-induced image (Fig. 2B) in the form of a contour plot with black lines. The most striking aspect of these figures is the correlation of enhanced photo-induced tunneling current with the edges of larger surface structures, that is at discontinuities in the surface topography. It can clearly be seen that the photo-induced image does not simply correlate with the height of large amplitude surface features but with specific topologies.

The far-field photo-induced signal detected through the STM tip arises from SPP-mediated ionization.[12] The principal features of the SPP-MPI process have been previously characterized.[12] Specifically, the expected non-linear power dependence (*i.e.*, cubic), asymmetric bias dependence, and pulse width limited temporal dependence in the far-field (*i.e.,* beyond the electron tunneling distance) for the SPP-MPI mechanism have all been clearly shown. The topography-reactivity correlation shown in Figure 2 can similarly be understood as a manifestation of SPP-mediated ionization from the surface at particular topographical features. The cubic power dependence[23] detected in the near-field (*i.e.,* within tunneling distance) demonstrates that the photo-induced signal is generated by a three-photon process. The nature of the signal is confirmed as a SPP-mediated multi-photon process given; (i) the photon energy of 1.6 eV compared with the work function of Ag of 4.3 eV, (ii) the sensitivity of the photo-induced signal to optical polarization and angular resonance, and (iii) the polarity of the tip-surface bias. The sharp features and discontinuities seen in the image yield the greatest enhancement. This is the anticipated result for SPP-MPI; the high local electromagnetic fields at the points of highest curvature, as in the case for oblate spheres,[8,11] result in enhanced local ionization yield.

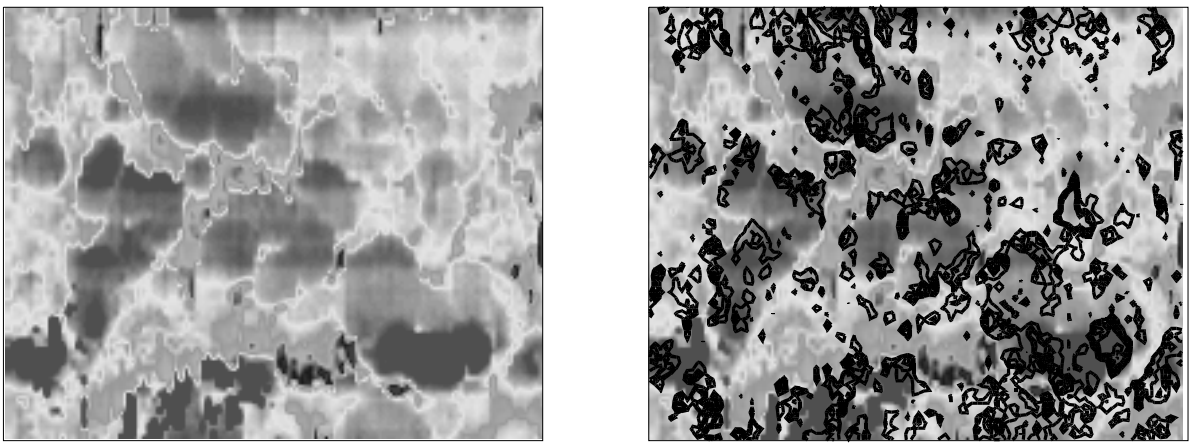

Figure 2. A. STM current-mode image of a 50 nm thick Ag metal film. The gray scale is in units of nanometers. The 1.0 x 0.8 μm image consists of 8,000 pixels from a scan step size of 10 nm in the X and Y directions. Set point (*i.e.*, DC) tunneling current = 100 pA, and bias = -10V to optimize electron collection. STM tip material is Pt:Ir. Scan rate is 2 pixels/second. B. SPP-MPI photo-induced reactivity image taken simultaneously with Fig 2A; overlay of topography (Fig. 2A, color) and SPP-MPI reactivity (Fig 2B, black contours) to facilitate correlating structure with reactivity. The color scale is in units of femtoamps. The signal is amplified by a custom pre-amplifier that has a 3 db band pass of 10 KHz and a gain of 10^9 V/A, and processed in a lockin amplifier (Stanford 850) that is referenced to a 3 KHz mechanical chopper modulation of the optical beams. Contours begin at 200 fA photo-induced current with additional contours spaced every 75 up to 500 fA.

Other topography- photo-induced reactivity (*i.e.*, SPP-mediated MPI) correlations have also been observed. The correlation of a very strong photo-induced signal with gaps and trenches is clearly evident. This result, again a manifestation of enhanced SPP-mediated reactivity at given surface features, confirms the predictions of Moskovits that gaps or trenches in the surface topography yield "even higher enhancements"[8] than other features. An analogous topology, prolate ellipsoids in close proximity, has been calculated to result in large local field enhancements that are even larger than for isolated spheroids. The latter enhancement is because of an additional SPP resonance occurring in the gap.[11] These results and the large photo-induced reactivity signal confirm that two very prolate ellipsoids (or their real world analog) separated by a small gap is an optimal topology for SES.[10]

A third type of correlation of surface photo-induced reactivity with surface topography has been identified. Locally rough features are found to give rise to large photo-induced reactivity signals. These results,[23] also agree well with the predictions from theory.[8,11] Phenomenologically, the roughness-reactivity correlations are understood within the framework of electromagnetic enhancement of SES. Surface roughness (random or structured) can be described as a 2-D Fourier superposition of optical gratings, where each grating and associated dispersion relation serves to couple photon energy into the film via SPP modes. Complicated interference patterns associated with the 2-D Fourier superposition of gratings result in areas of spatially localized field enhancements that have been referred to as localized surface plasmon polaritons (LSP).[9] The origin of the observed enhancements at sharp discontinuities and gaps, Figures 2 and 3, can also be understood within the framework of LSP excitation.

The temporal response associated with SPP-MPI can be established using a pump-probe scheme; *i.e.*, detection of the local ionization response as a function of the temporal separation between two excitation pulses. The CORSTM pump-probe response shown in Figure 3 is dominated by the ultrafast pulse width limited peak at the pump-probe zero of time with a smaller amplitude component extending well beyond the pulse duration that decays to a baseline level of ~325 fA. The longer decay component is exponential with a time constant of 500-700 fs, orders of magnitude faster than the timescale for thermal expansion and diffusion of Ag films.[24]

The ultrafast peak can be understood as arising from an instantaneous three photon ionization response. Specifically, with temporally and spatially overlapped pulses of approximately equal intensity, I, the signal for a three photon process is proportional to $(2I)^3$. The signal at longer delay times, after populated states intermediate between the Fermi and the vacuum levels have decayed, will be proportional to $2I^3$. The observed result of Figure 3 shows a long time signal that is a factor of 4 lower than the time zero response.

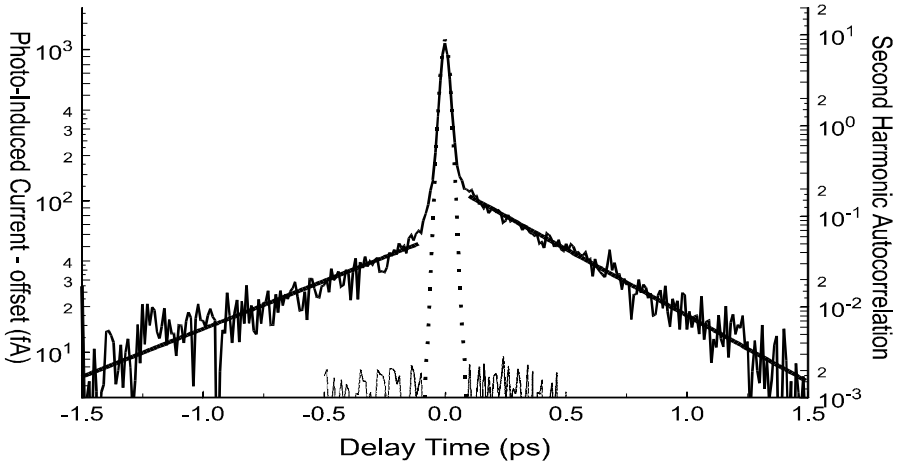

Figure 3. Semi-log plot of the temporal SPP-MPI data (solid line) and second harmonic autocorrelation (dashed line). A 325 fA offset has been subtracted from the SPP-MPI data. The long time exponential components (straight lines fitted through data) have temporal decay constants of 680 and 490 fs. This temporal response of the SPP-MPI signal was obtained with an optical excitation repetition rate of 50 KHz and with the STM tip piezoelectrically withdrawn 25 ± 5 nm from the surface in order to enhance the signal to noise ratio by minimizing the tunneling current and its 1/f noise. Even with a withdrawn tip the spatial region from which the ionization response is being detected is still less that the diffraction limit of $\lambda/2$ established by the optical excitation wavelength.

The 500-700 fs decays are indicative of the existence of intermediate electronic states with finite lifetimes and represent excited state population relaxation dynamics. An all optical measurement of the thermalization of hot electrons created by SPP excitation in Ag films determined that this process occurs with an exponential time constant of 670(70) fs.[24] The decays in Figure 3 are therefore attributed to the relaxation of hot electrons, resulting from SPP excitation, by inelastic electron-phonon collisions. Resolution of these hot electron dynamics, not seen in far-field MPI measurements,[12,13] is believed to be a consequence of improved near-field collection efficiency and higher peak pulse energy. The temporal asymmetry of the decay times is attributed to small asymmetries in the alignment, focusing conditions and spatial overlap of the beams relative to the STM tip. These time resolved results demonstrate the importance of using ultrafast excitation to generate the CORSTM MPI response by coupling energy directly into the electrons without allowing time for thermalization of the lattice. Further studies with asymmetric pulse intensities are being conducted.

4. DISCUSSION

It is important to rule out other causes for the photo-induced signal. First, high frequency 1/f noise from the resistive tip-sample junction and the pre-amp must be considered. It has been found that 1/f noise directly correlates with the amplitude of the surface features; that is, when the tunneling current is large the high frequency noise is also large. However, *the photo-induced reactivity images of Figure 2 and other data not shown correlate with surface topology and do not simply correlate with the magnitude of the tunneling current signal*. Second, the low repetition rate low pulse energy experimental conditions rule out a bulk lattice thermal effect as does the temporal response of Figure 3.[25] Third, the influence of adsorbates on the correlated structure-reactivity measurements must also be considered.

It is well known that the work function of a metal can decrease as a result of adsorption of species such as H_2O and pyridine.[9,26] In addition, adsorbates have been shown to enhance photoemission yields from Au and Ag films.[27] However, adsorbates are thought not to be the dominant mechanism responsible for the results presented herein for several reasons. First, even if adsorbates were preferentially bound at edges, gaps and roughness one might expect maximum enhancements of at most 100-fold.[28] However, the SPP-MPI images show signal enhancements at different surface features as high as 2000-fold above the noise level. Second, since the experiments were performed under ambient conditions the most likely adsorbate is H_2O. In fact, one would expect the adsorption of many layers of H_2O that have significant mobility given the room temperature experimental conditions. Thus, the coverage should be uniform and not preferentially located at edges, gaps, or roughness features.[29] Third, oxidation may also be a significant surface contamination. However, the oxidation of silver has been found to lower the work function to only 4.06 eV.[30] A drop of this small magnitude would still require three photons for ionization (the measured power dependence). Even if preferentially located at step edges or defect sites, oxides would not be expected to provide significant enhancements in the total yield of photoemission that is detected here. In summary, neither systematic artifacts, thermal expansion, or adsorbates can account for the observed local enhancements. Rather, based on the strong correlation with predictions of electromagnetic theory and the fact that CORSTM responses from rough Au surfaces have been obtained,[23] the observed enhancements can be understood as being the result of the high electromagnetic fields associated with localized surface plasmons.

5. CONCLUSIONS

This paper has described a general technique, CORSTM, to study the correlation of surface photo-reactivity with local surface structure by obtaining local dynamical information with approximately 10 fs time resolution and better than 10 nm spatial resolution. CORSTM has been shown to be able to visualize the topographical dependence of electromagnetic enhancements relevant for surface enhanced spectroscopy. It has been experimentally demonstrated that the best topology for SES are gaps and sharp discontinuities. The theoretically predicted relative local field enhancements due to various surface topologies have been experimentally verified in the present work.

Finally, the temporal dynamics of surface plasmon polaritons have been obtained in spatially localized measurements. The relaxation of the collective SPP mode on rough surfaces occurs via an ultrafast response. Subsequent exponential decays in the localized pump-probe signal reflect the thermalization of hot electrons. These measurements and the characterization of localized structure-reactivity correlations are only possible through the use of ultrashort pulsed excitation that (i) facilitates discrimination of the nonlinear signal, (ii) allows establishing the temporal dynamics and (iii) prevents thermalization on the time scale of the pulse.

This method has important implications for investigating chemical reactivity induced by electronic transitions.[31] The structure-function correlations that have been revealed by CORSTM measurements are being extended to study SPP-MPI on periodically ordered surfaces[32] to further test electromagnetic theories. In addition, this technique can be used to study electron injection into chemical systems from structured surfaces.[33,34] The use of CORSTM to determine an ideal substrate topography to maximize SPP-MPI will open up new opportunities for the study of electron injection into liquids.[35] The observed localized SPP-MPI response and the potential for patterning local field variations on surfaces by design will have many interesting consequences in initiating chemical reactions (*e.g.*, polymerization) at these interfaces and technologically important problems including organic LED's where the first step is electron and / or hole injection into a polymer overlayer.

6. ACKNOWLEDGEMENTS

We thank The University of Chicago NSF-supported MRSEC and the David and Lucile Packard Foundation for financial support. We also acknowledge partial support from the NSF National Young Investigator Program (CHE9357424), the Alfred P. Sloan Foundation, and a Camile Dreyfus Teacher-Scholar Award. We thank Yish-Hann Liau and Mary Kulberg for assistance in preparation of this paper.

7. REFERENCES

1. J. I. Pascual, J. Méndez, J. Gómez-Herrero, A. M. Baró, N. Garcia, U. Landman, W. D. Luedtke, E. N. Bogachek, H.-P. Cheng, *Science*, **267**, 1793, 1995.

2. H. Raether, *Surface Plasmons*, Springer-Verlag, Berlin, 1988.

3. R. P. Van Duyne, J. C. Hulteen, D. A. Treichel, *J. Chem. Phys.*, **99** (3), 2101, 1993.

4. B. Rothenhäuser, C. Duschl, W. Knoll, *Thin Solid Films*, **159**, 323, 1988; C. R. Lawrence, N. J. Geddes, D. N. Furlong, J. R. Ambles, *Biosensors Bioelectronics,* **11** (4), 389, 1996.

5. S. I. Bozhevolnyi, I. I. Smolyaninov, A. V. Zayats, *Phys. Rev. B*, **51**, 17916, 1995; M. Specht, J. D. Pedarnig, W. M. Hechel, T. W. Hänsch, *Phys. Rev. Lett.*, **68**, 476, 1992.

6. R. G. Freeman, K. C. Graber, K. J. Allison, R. M. Bright, J. A. Davis, A. P. Guthrie, M. B. Hommer, M. A. Jackson, P. C. Smith, D. G. Walter, M. J. Natan, *Science*, **267**, 1629, 1995; M. J. Feldstein, C. D. Keating, Y. H. Liau, M. J. Natan, N. F. Scherer, *J. Am. Chem. Soc.*, in press, 1997.

7. M. Fleishmann, P. J. Hendra, A. J. McQuillan, *Chem. Phys. Lett*., **26**, 163, 1974.

8. M. Moskovits, *Rev. Mod. Phys.*, **57** (3), 783, 1985 and references therein.

9. C. Douketis, V. M. Shlaev, T. L. Haslett, Z. Wang, M. Moskovits, *J. Elec. Spec. Rel. Phen.*, **64**/**65**, 167-175, 1993.

10. T. Xiao, Q. Yi, L. Sun, *J. Phys. Chem. B.*, **101**, 632 (1997). S. R. Emory, S. Nie, *Science*, **275**, 102, 1997.

11. J. Gersten, A. Nitzan, *J. Chem. Phys.*, **73** (7), 3023, 1980; U. Laor, G. C. Schatz, *J. Phys. Chem.*, **76** (6), 2888, 1982; H. Metiu, P. Das, *Ann. Rev. Phys. Chem.*, **35**, 507, 1984 and references therein.

12. M. J. Feldstein, P. Vöhringer, W. Wang, N. F. Scherer, *J. Phys. Chem.*, **100** (12), 4739, 1996.

13. T. Tang, T. Srinivasan-Rao, J. Fischer, *Phys. Rev. B.*, **43** (11), 8870, 1991.

14. Möller *et al*., *J. Vac. Sci. Tech. B.* **9** (2), 506, 1991.

15. H. Q. Nguyen, P. H. Cutler, T. E. Feuchtwang, Z.-H. Huang, Y. Kuk, P. J. Silverman, A. A. Lucas, T. E. Sullivan, *IEEE Trans on Electron Devices*, **36**, 2671, 1989.

16. Bozhevolnyi *et al.*, *Phys. Rev. B.*, **51**(24), 17916, 1995.

17. W. Wang, M. J. Feldstein, N. F. Scherer, *Chem. Phys. Lett.*, **262**, 573, 1996.

18. J. Grafström, J. Kowalski, R. Neumann, O. Probst and M. Wörtge, *J. Vac. Sci. Tech.*, **B9**, 568, 1991.

19. D. C. Arnett, P. Vöhringer, N. F. Scherer, *J. Am. Chem. Soc.*, **117** (49), 12262, 1995.

20. G. Bining, H. Rohrer, *Helv. Phys. Acta,* **55**, 726, 1982.

21. Digital Instruments, Nanoscope II Instruction Manual.

22. J. A. Stroscio, D. M. Eigler, *Science*, **254**, 1319, 1991.
23. M. J. Feldstein, N. Scherer, submitted to *Phys. Rev. Lett.*, 1998.

24. R. H. M Groenveld, R. Sprik, A. Lagendijk, *Phys. Rev. Lett.*, **67** (7), 784, 1990.

25. It has been possible to exclude thermal mechanisms, such as tip expansion, as the predominant photo-induced signal generation mechanism due to the following: (i) the cubic power dependence, (ii) the average incident power is only on the order of 1-10 W/cm^2, depending upon laser repetition rate, and is 1-2 orders of magnitude lower than in Reference **Error! Bookmark not defined.**, while the peak power is extremely high. (iii) less than 30% of the incident light is absorbed by the Ag film due to the SPP resonance and focusing conditions, therefore, the net energy absorbed by the film is only on the order of or less than 1 W/cm^2, and (iv) the measured time dependence emphasizes the importance of ultrafast electronic excitation as opposed to a slow time-integrated thermal background signal.

26. C.-W. Kim, J. C. Villagrá, U. Even, J. C. Thompson, *J .Chem. Phys.*, **94** (4), 3974-7, 1991.

27. U. Even, K. A. Holcomb, C. W. Snyder, P. R. Antoniewicz, J. C. Thompson, *Surf. Sci. Lett.*, **165**, L35-40, 1986.

28. The largest reported enhancement attributed to an adsorbate in photoemission from Ag films was 100-fold for cesium, and only 4-20-fold for molecular adsorbates with electron donating groups and dipoles aligned normal to the surface such as nitrobenzene, pyrazine, and pyridine.[Error! Bookmark not defined.]

29. Douketis *et al.*[9] found no additional reduction of Ag's work function beyond a maximum drop of 0.6 eV with additional H_2O dosing after 5L (about 5 monolayers) had been applied. Moreover, no significant increase in the photoemission yield was reported for this system.

30. M. Nilges, J. H. Freed, *Chem. Phys. Lett.*, **85** (5,6), 499, 1982.

31. J. A. Misewich, T. F. Heinz, M. B. Newns, *Phys.Rev.Lett.*, **68** (25), 3737, 1992.

32. M. Winzer, M. Kleiber, N. Dix, R. Wiesendanger, *Appl. Phys. A*, **63**, 617, 1996; J. C. Hulteen, R. P. Van Duyne, *J. Vac. Sci. Tech. A*, **13**, 1553, 1995.

33. A. Kadyshevitch, R. Naaman, *Phys. Rev. Lett.*, **74** (17), 3443, 1995.

34. Y.-H. Liau and N. F. Scherer, submitted to *Phys. Rev. Lett.*, 1997.

35. T. W. Scott, *J. Phys. Chem.*, **90**, 1739, 1986.

J.I. Pascual, J. Méndez, J. Gómez-Herrero, A.M. Baró, N. Garcia, U. Landman, W.D. Luedtke, E.N. Bogachek, H.-P. Cheng, *Science*, **267**, 1793 (1995).

H. Raether, *Surface Plasmons*, Springer-Verlag, Berlin (1988).

R.P. Van Duyne, J.C. Hulteen, D.A. Treichel, *J.Chem.Phys.*, **99**(3), 2101 (1993).

B. Rothenhäuser, C. Duschl, W. Knoll, *Thin Solid Films*, **159**, 323 (1988); C.R. Lawrence, N.J. Geddes, D.N. Furlong, J.R. Ambles, *Biosensors lectronics,* **11**(4), 389 (1996).

S.I. Bozhevolnyi, I.I. Smolyaninov, A.V. Zayats, *Phys.Rev.B*, **51**, 17916 (1995); M. Specht, J.D. Pedarnig, W.M. Hechel, T.W. Hänsch, *Phys.Rev.Lett.*, (1992).

R.G. Freeman, K.C. Graber, K.J. Allison, R.M. Bright, J.A. Davis, A.P. Guthrie, M.B. Hommer, M.A. Jackson, P.C. Smith, D.G. Walter, M.J. Natan, *ıce*, **267**, 1629 (1995); M.J. Feldstein, C.D. Keating, Y.H. Liau, M.J. Natan, N.F. Scherer, *J.Am.Chem.Soc.*, in press (1997).

M. Fleishmann, P.J. Hendra, A.J. McQuillan, *Chem.Phys.Lett*, **26**, 163 (1974).

M. Moskovits, *Rev.Mod.Phys.*, **57**(3), 783 (1985) and references therein.

. Douketis, V.M. Shlaev, T.L. Haslett, Z. Wang, M. Moskovits, *J.Elec.Spec.Rel.Phen.*, **64**/**65**, 167-175 (1993).

T. Xiao, Q. Yi, L. Sun, *J.Phys.Chem.B.*, **101**, 632 (1997). S.R. Emory, S. Nie, *Science*, **275**. 102 (1997).

J. Gersten, A. Nitzan, *J.Chem.Phys.*, **73**(7), 3023 (1980); U. Laor, G.C. Schatz, *J.Phys.Chem.*, **76**(6), 2888 (1982); H. Metiu, P. Das, *Ann.Rev.Phys.Ch* 607 (1984) and references therein.

M.J. Feldstein, P. Vöhringer, W. Wang, N.F. Scherer, *J.Phys.Chem.,* **100**(12), 4739, (1996).

T. Tang, T. Srinivasan-Rao, J. Fischer, *Phys.Rev.B.*, **43**(11), 8870 (1991).

Möller et al., *J.Vac.Sci.Tech.B.*, **9**(2), 506 (1991).

Cutler

Bozhevolnyi *et al.*, *Phys.Rev.B.*, **51**(24), 17916 (1995)].